nature chemistry

Article

https://doi.org/10.1038/s41557-023-01231-z

D_3^+ formation through photoionization of the molecular D_2–D_2 dimer

Received: 28 July 2022

Accepted: 4 May 2023

Published online: 1 June 2023

Check for updates

Yonghao Mi[1] ✉, Enliang Wang[2,3] ✉, Zack Dube[1], Tian Wang[1], A. Y. Naumov[1], D. M. Villeneuve[1], P. B. Corkum[1] & André Staudte[1] ✉

The H_2–H_2 molecular dimer is of fundamental importance in the study of chemical interactions because of its unique bonding properties and its ability to model more complex systems. The trihydrogen cation H_3^+ is also a key intermediate in a range of chemical processes in interstellar environments, such as the formation of various organic molecules and early stars. However, the unexpected high abundance of H_3^+ in molecular clouds remains challenging to explain. Here using near-infrared, femtosecond laser pulses and coincidence momentum imaging, we find that the dominant channel after photoionization of a deuterium molecular dimer (D_2–D_2) is the ejection of a deuterium atom within a few hundred femtoseconds, leading to the formation of D_3^+. The formation mechanism is supported and well-reproduced by ab initio molecular dynamics simulations. This pathway of D_3^+ formation from ultracold D_2–D_2 gas may provide insights into the high abundance of H_3^+ in the interstellar medium.

The trihydrogen cation (H_3^+), structured by three protons and two electrons, is one of the most abundant molecular ions in the universe. As a proton donor, H_3^+ initiates most chemical reactions in interstellar space, making substantial contributions to the formation of almost all molecules[1–3]. H_3^+ can also cool the condensing gases in interstellar clouds and therefore plays a vital role in the formation of stars. Following ionization of interstellar H_2 by cosmic rays, the subsequent ion–molecule reaction ($H_2 + H_2^+ \rightarrow H_3^+ + H$) is considered to be the main pathway of H_3^+ production in the interstellar medium. In 1996 and 1998, H_3^+ was detected in dense[4] and in diffuse interstellar molecular clouds[5]. Surprisingly, the detected H_3^+ column density in diffused clouds is a few orders of magnitude higher than the expected value derived from a model that considers the production and destruction rates of H_3^+ in those diffused clouds[1]. This is known as the H_3^+ problem, and the enigma of the pervasive H_3^+ in the interstellar medium has been challenging to understand.

When first discovered by J. J. Thomson with a prototypic mass spectrometer in 1911[6], H_3^+ was produced in an electrical discharge in H_2 gas via the ion–molecule reaction between H_2^+ and H_2 (ref 7). H_3^+ can also be produced by doubly ionizing small organic molecules using electron- or ion-impact ionization[8–11] or photoionization with intense laser fields[8,12–21]. This formation mechanism has been attributed to H_2 roaming, and the timescale of the process has been investigated[11,13,18–21]. Recently, the formation of H_3^+ from nanoparticle-adsorbed water molecules has been observed[22].

As the most abundant element in the universe, huge amounts of atomic hydrogen exist in our galaxy in warm (10^3–10^4 K) and cool (50–100 K) regions, while cold (10–30 K) regions are considered to be dominated by dense clouds of molecular hydrogen[23]. The presence of H_2 in these clouds has been attributed to the catalytic action of dust particles[24]. The same mechanism could allow the formation of H_2 dimers. H_2 dimers, with an actual binding energy of ~3 cm^{-1}, are among the most weakly bound dimers in nature. H_2 dimers are thus elusive to spectroscopic detection, yet they have been found in the upper atmospheres of Jupiter and Saturn[25–28].

In this Article, we propose a pathway of H_3^+ formation under laboratory conditions, which proceeds through single ionization of an H_2 dimer (H_2–H_2) and a subsequent proton transfer process in the dimer. Throughout this work, deuterium molecules (D_2) are used in calculations and experiments. This choice is made for experimental reasons:

[1]Joint Attosecond Science Laboratory, National Research Council and University of Ottawa, Ottawa, Ontario, Canada. [2]Hefei National Research Center for Physical Sciences at the Microscale and Department of Modern Physics, University of Science and Technology of China, Hefei, China. [3]Max-Planck-Institut für Kernphysik, Heidelberg, Germany. ✉e-mail: ymi@uottawa.ca; elwang@ustc.edu.cn; andre.staudte@nrc-cnrc.gc.ca

https://doi.org/10.1038/s41557-023-01231-z

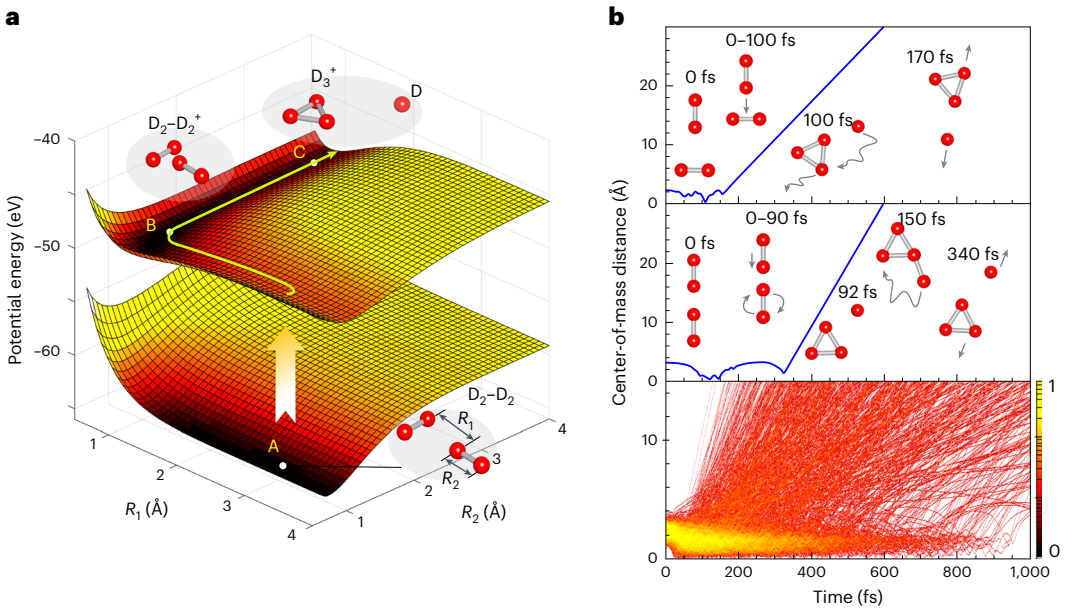

Fig. 1 | PES and trajectory simulations. a, Calculated PES of a D_2 dimer and the schematic pathway of D_3^+ formation. The calculated PES indicates that D_2–D_2^+ is not a stable molecular ion and it will continue dissociating into a D_3^+ and a deuterium atom. **b**, Simulation results of the time-dependent distance between D_3^+ and D for a T-shaped (top) and a parallel-aligned (middle) D_2 dimer, and simulated trajectories (centre-of-mass distance between D_3^+ and D) of D_3^+ formation for 892 D_2 dimer cations (bottom). The simulations display the real-time trajectories of D_2–D_2 dissociation after single ionization. These results show that D_3^+ formation from D_2–D_2 is an efficient pathway.

by measuring D_3^+ instead of H_3^+, we can avoid the ambiguity of the H_3^+ mass spectrum peak with the ever-present contaminant HD^+. Moreover, having the exact same electronic structure, D_2–D_2 only differs from H_2–H_2 in the reduced speed of the nuclear dynamics, making it also more amenable for our pump–probe scheme.

Results and discussion

Potential energy surface of D_2–D_2

We first calculated the potential energy surface (PES) of D_2–D_2. Figure 1a shows the coordinates R_1 and R_2, which represent the centre-of-mass distance between one D_2 molecule and a deuteron of the other D_2 molecule, and the internuclear distance of the other D_2 molecule, respectively. Point A on the lower PES shows the stationary point (equilibrium geometry) of the ground state of D_2–D_2. When an electron is removed, the molecular dimer is projected onto the ground state of D_2–D_2^+ and moves along the pathway marked by the yellow line. The D_2–D_2^+ ground state has an energy minimum (point B) with a potential energy barrier of ~0.25 eV (details are provided in Supplementary Section 1), which is lower than the potential energy of the Franck–Condon region. Therefore, D_2–D_2^+ is not a stable molecular ion and dissociates into a D_3^+ ion and a deuterium atom (point C).

Trajectory simulation

With the knowledge of this possible pathway, we carried out an ab initio molecular dynamics simulation to extract the temporal information of the D_3^+ formation. One thousand trajectories were simulated, and 892 of these led to D_3^+ formation. Figure 1b shows the simulated centre-of-mass distance between D_3^+ and D as a function of time. In the top two panels of Fig. 1b we show two typical trajectories for the T-shape and parallel-aligned D_2 dimer. These two trajectories start from their respective equilibrium geometries without any initial internal energy. For ionization of a T-shape dimer, the D_2^+ moves towards the D_2 and a deuteron is attracted by the D_2. At 100 fs, three deuterons start bonding together, while all four deuterons are still close to each other. The produced D_3^+ and D separate after 170 fs, as indicated by the trajectory in the top panel of Fig. 1b. For a parallel-aligned dimer, the formation process is the same as that of the T-shape dimer. However, the formation time is about twice as long (Fig. 1b, middle panel). We also simulated the formation process of D_3^+ with the initial geometry of an X-shaped D_2 dimer (Extended Data Fig. 1). The complete dynamics of D_3^+ formation for all three geometries of the dimer is provided in Supplementary Videos 1–3. The bottom panel of Fig. 1b shows the simulated time-dependent trajectories (centre-of-mass distance between D_3^+ and D) for the 892 dimer cations leading to D_3^+.

For comparison, the simulation was also performed on H_2 dimers. The time-dependent centre-of-mass distances for T-shaped, parallel-aligned and X-shaped H_2 and D_2 dimers are shown in Extended Data Fig. 1. To estimate the branching ratio of H_3^+ formation, we simulated 593 trajectories of H_2–H_2^+. Of these, 493 ended up with the H_3^+ + H channel, as shown in Extended Data Fig. 2a. The obtained branching ratio of 83.1% is close to that of the D_3^+ (89.2%).

Experimental observation of D_3^+ formation

Next, we turn to the experiment for the formation of trihydrogen cations from hydrogen molecular dimers using D_2. The experiment was performed in a cold-target recoil-ion momentum spectroscopy (COLTRIMS) reaction microscope[29]. The D_2 dimers were prepared in a cold molecular beam via supersonic expansion of D_2 gas into a high-vacuum (10^{-11} mbar) chamber through a 10-µm nozzle and a skimmer (Fig. 2a). Details of the experimental set-up are provided in Methods.

The time-of-flight (TOF) spectrum of the photoions was measured. As shown in Fig. 2b, the dominant peak is D_2^+ (TOF ≈ 2,250 ns), which is produced by single ionization of the D_2 molecules in the gas jet. The multiple peaks centred at ~1,590 ns in the spectrum correspond to D^+ ejected during dissociation of D_2^+. The sharp peak at 1,950 ns is HD^+ originating from the HD in the D_2 gas cylinder. Centred at ~2,750 ns, a broad peak with a mass-to-charge ratio of 6, corresponding to D_3^+, was observed. This evidences the observation of D_3^+ produced from D_2–D_2.

To investigate the breakup mechanism of D_2–D_2, the photoion–photoion coincidence (PIPICO) spectrum was recorded (Fig. 3). The sharp diagonal lines in this figure indicate that the first and second ions originate from a two-body fragmentation of a molecule.

https://doi.org/10.1038/s41557-023-01231-z

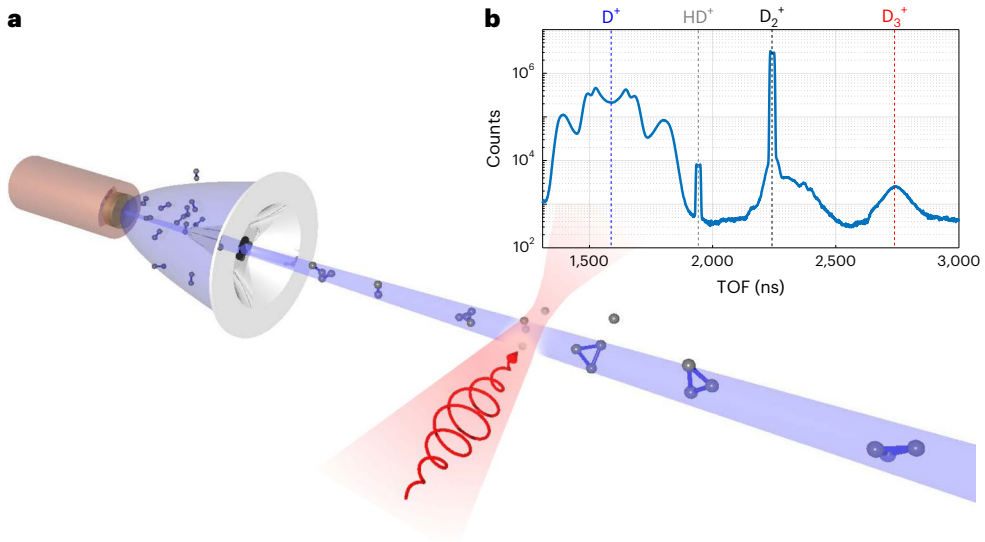

Fig. 2 | Sketch of the experimental set-up and TOF spectra. a, The D_2 dimers (D_2–D_2) are generated in the supersonic expansion of D_2 gas through a precooled (60 K) nozzle and a skimmer. The dimers are ionized by 25-fs, 790-nm, circularly polarized laser pulses. **b**, Measured TOF spectrum of the photoions. The blue, grey, black and red dashed lines specify the centre TOFs of D^+, HD^+, D_2^+ and D_3^+ photoions, respectively. The observation of the D_3^+ peak evidences D_3^+ production from D_2–D_2.

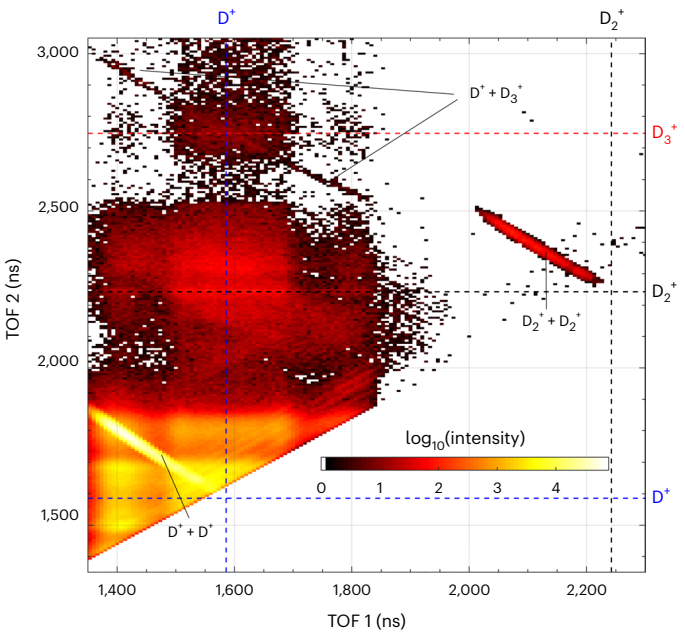

Fig. 3 | Measured PIPICO spectrum. TOFs 1 and 2 refer to the measured TOFs of the first and second photoions. The centre TOFs of D^+, D_2^+ and D_3^+ are shown by blue, black and red dashed lines, respectively. The sharp diagonal lines show that the first and second ions originate from dissociation of a molecule. The coincidence measurement between D^+ and D_3^+ confirms that the D_3^+ ion is a product of the breakup of a D_2–D_2 dimer.

The centre TOFs of D^+, D_2^+ and D_3^+ are marked with dashed lines for better characterization of the coincidence between these photoions. As shown in Fig. 3, besides the $D^+ + D^+$ correlation, which indicates the Coulomb explosion of D_2 molecules, we also observed $D_2^+ + D_2^+$ and $D^+ + D_3^+$ correlations. These two channels originate from the double ionization and subsequent breakup of D_2 dimers. The correlation on the PIPICO spectrum confirms this pathway of D_3^+ formation. We note that the probability of double ionization is much smaller than that of single ionization. Therefore, the yield of $D^+ + D_3^+$ is much lower compared to the yield of D_3^+ that is produced from single ionization of D_2–D_2 (D_2–$D_2^+ \rightarrow D_3^+ + D$). In this experiment, D_2–D_2^+ was not observed in the TOF spectrum. This agrees well with the simulation results: D_2–D_2^+ is not stable and will dissociate into D_3^+ and D.

Dynamics of D_3^+ formation

Is it possible to measure the timescale of the D_3^+ formation process? To answer this question, we designed a pump–probe experiment in which the circularly polarized laser pulse (3×10^{14} W cm^{-2}) serves as the pump pulse, and a delayed, weak pulse (5×10^{13} W cm^{-2}) with linear polarization was introduced as the probe. The circularly polarized pump pulse triggers single ionization of D_2–D_2 while minimizing alignment-selective ionization. Furthermore, circular polarization suppresses recollision-induced processes such as double ionization. Note that the pump pulse removes an electron via a multiphoton ionization process. This suggests that the timescale of the dissociation may be affected by vibrational excitation of the molecules in the dimer. However, because the pulse duration of the pump and the probe (25 fs) is much shorter than the vibrational period of the two D_2 molecules in D_2–D_2 (~921.4 fs from the calculation), the ionization occurs so quickly that it can be considered a vertical ionization, which is analogous to a single-photon ionization. Compared to the pump pulse, the linearly polarized probe pulse is too weak to ionize D_2–D_2; however, it can work as a disruptive pulse[20], which perturbs the intermediate D_2–D_2^+ cation either by dissociating or by secondary ionization and thereby probes the dissociation dynamics.

Figure 4a shows the yield of D_3^+ as a function of the pump–probe delay for a time-delay range between −250 and 1,000 fs. The positive and negative delays indicate that the pump pulse comes before and after the probe pulse, respectively. When the delay is between −150 and 150 fs, the constructive interference between the two pulses produces a higher peak intensity. Thus, the ionization rate of D_2–D_2 and thus the yield of D_3^+ peak in this time window. However, the yield of D_3^+ increases exponentially from 150 to 1,000 fs. The exponential shape can be understood qualitatively by the following D_3^+ formation dynamics: when an electron is removed from a D_2–D_2 at time zero, D_2–D_2^+ starts to dissociate. In the first 100 fs, the deuterons are still in the vicinity of each other. The weak probe pulse can destroy the rearrangement process and prevent the system from evolving to a D_3^+ and a D atom.

https://doi.org/10.1038/s41557-023-01231-z

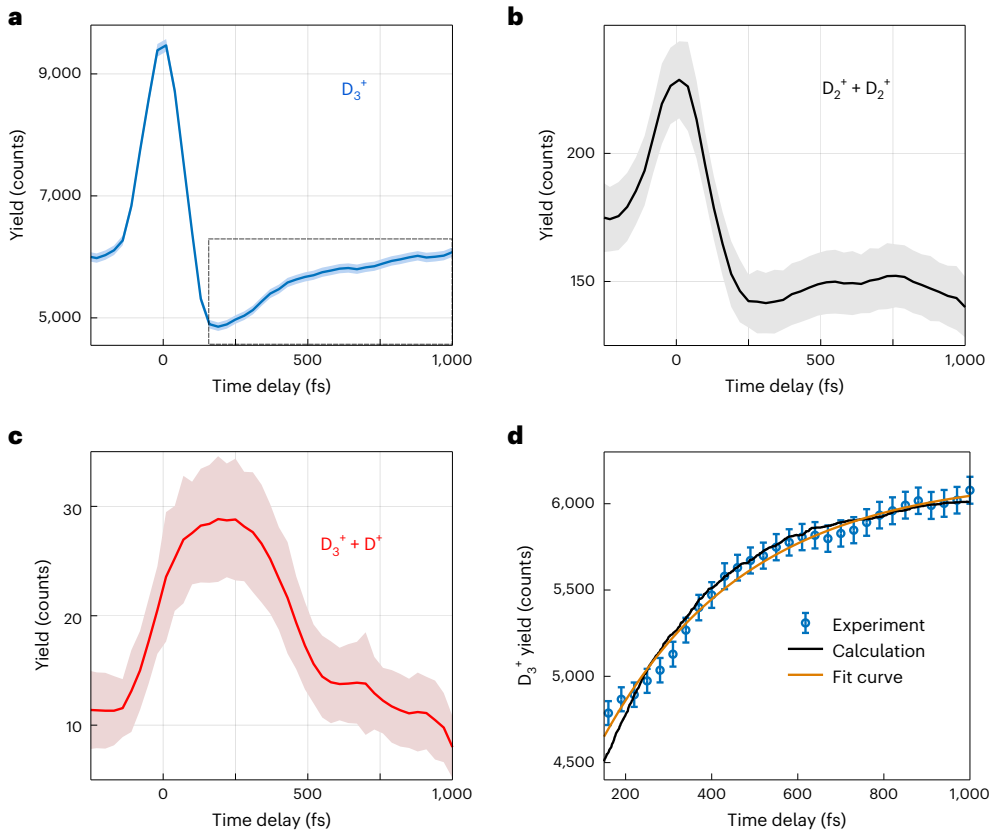

Fig. 4 | Experimental results of the time-dependent yields for different channels. a–c, Yield of D_3^+ (**a**), $D_2^+ + D_2^+$ (**b**) and $D_3^+ + D^+$ (**c**) as a function of pump–probe time delay (shaded area given by error bands). These error bands are standard deviations (s.d.) of the corresponding number of counts at each time delay. **d**, Experiment, calculation and fit curve of the time-dependent D_3^+ yield for the range between 150 and 1,000 fs. The experimental data are presented as mean values ± s.d. The box in **a** shows the yield of D_3^+ between 150 and 1,000 fs (outside the temporal overlap between the pump and probe pulses). In this region, we fit the D_3^+ yield with a growth function and extract the formation time $\tau = 330 \pm 55$ fs. The time-dependent yields of different channels of D_2–D_2 dissociation indicate that chemical reactions between two D_2 molecules in an isolated bimolecular system can be controlled by laser pulses.

However, when the D_3^+ has already been formed at larger delays (that is, >400 fs), the probe pulse is not sufficiently intense to interrupt this process and thus the D_3^+ yield recovers as the delay increases. When the weak probe pulse arrives first, it is not strong enough to ionize D_2–D_2. The D_2–D_2 ionized by the late-coming pump pulse leads to D_3^+ in any case. Therefore, no substantial time-dependent yield of D_3^+ was observed at negative delays.

Next, we investigate the ultrafast dissociation dynamics of the double-ionization channels. We show the time-resolved yields of $D_2^+ + D_2^+$ and $D^+ + D_3^+$ in Fig. 4b,c, respectively. The $D_2^+ + D_2^+$ yield does not show a distinct time-dependent variation outside the temporal overlap (>150 fs). However, the yield of $D^+ + D_3^+$ exhibits a maximum around 200 fs, when the yield of the $D + D_3^+$ channel is minimized.

Comparing the yields of the two double-ionization channels with the time-resolved D_3^+ yield, we find that the suppression of the D_3^+ yield within the first few hundred femtoseconds can be at least partially explained with an enhanced yield of $D_3^+ + D^+$. However, in view of the overall low probability for double ionization (due to the low-intensity probe pulse), a dissociation of the D_2–D_2^+ into $D^+ + D + D_2$ via bond softening[30] is probably the dominant pathway induced by the probe pulse. This bond softening is caused by a very strong a.c. Stark shift of the highly polarizable molecular ion. Details of the suppression of the D_3^+ yield are discussed in Supplementary Section 5.

We now compare our experimental results with the calculation. For delay times smaller than 150 fs, the overlap of the pump and probe pulses causes an enhanced yield in all channels. Hence, we concentrate our attention on the time window between 150 and 1,000 fs. In Fig. 4d the measured D_3^+ yield, shown by blue circles, starts out from a minimum and then grows to asymptotically recover to the value at negative time delays. We fit the D_3^+ yield with the growth function $Y(t) = a(1 - e^{-t/\tau}) + Y_0$, where a and Y_0 are the amplitude and the offset of the D_3^+ yield, and τ is the formation time of D_3^+. Using this fit function, we extract the formation time $\tau = 330 \pm 55$ fs. The theoretical D_3^+ yield (black line) was obtained by projecting the trajectories in the bottom panel of Fig. 1b with a centre-of-mass distance larger than 8.0 a.u. (4.2 Å, which excludes most of the oscillation structures) on the time-delay axis. To facilitate comparison with the experimental data, the theoretical results were scaled accordingly. As shown in Fig. 4d, the theoretical D_3^+ yield is in good agreement with the experimental data (blue circles) and the fit curve (orange line). With the same method as for the calculation for D_2–D_2, we also calculated and fitted the time-dependent yields of H_3^+ from single ionization of H_2–H_2 as a function of time. The formation was determined to be 169.5 fs. These calculation results for H_2 dimers are shown in Extended Data Fig. 3.

Conclusion

In conclusion, we have demonstrated in both theory and experiment that the trihydrogen cation can be produced via single ionization of a hydrogen molecular dimer. Taking a different perspective, the dimer represents a chemical reaction in waiting, which is triggered by the arrival of the ionizing pump pulse. Upon ionization, the D_2–D_2^+ begins the transition to $D_3^+ + D$. The probe pulse modifies the PES, leading the system away from the dominant reaction pathway. This

is an example of the dynamic Stark control of a chemical reaction[31]. The pump–probe experiment demonstrated that chemical reactions on isolated bimolecular system can be controlled and steered by a weak laser pulse.

Although H_2 dimers will not be subjected to intense laser pulses in interstellar space, the ionization dynamics can be expected to proceed very similarly for high-energy photons (cosmic rays) due to the electronic simplicity of H_2. Although the detection of H_2 dimers in the interstellar medium is challenging due to their weak bond, the observation of H_2 dimers in the atmospheres of Jupiter and Saturn could indicate that the contribution of hydrogen dimers to the formation of H_3^+ has been neglected.

Online content

Any methods, additional references, Nature Portfolio reporting summaries, source data, extended data, supplementary information, acknowledgements, peer review information; details of author contributions and competing interests; and statements of data and code availability are available at https://doi.org/10.1038/s41557-023-01231-z.

References

1. Oka, T. Interstellar H_3^+. *Proc. Natl Acad. Sci. USA* **103**, 12235–12242 (2006).
2. Geballe, T. R. & Oka, T. A key molecular ion in the universe and in the laboratory. *Science* **312**, 1610–1612 (2006).
3. Oka, T. Interstellar H_3^+. *Chem. Rev.* **113**, 8738–8761 (2013).
4. Geballe, T. R. & Oka, T. Detection of H_3^+ in interstellar space. *Nature* **384**, 334–335 (1996).
5. McCall, B. J., Geballe, T. R., Hinkle, K. H. & Oka, T. Detection of H_3^+ in the diffuse interstellar medium toward Cygnus OB2 No. 12. *Science* **279**, 1910–1913 (1998).
6. Thomson, J. J. XXVI. Rays of positive electricity. *London Edinburgh Dublin Philos. Mag. J. Sci.* **21**, 225–249 (1911).
7. Hogness, T. R. & Lunn, E. G. The ionization of nitrogen by electron impact as interpreted by positive ray analysis. *Phys. Rev.* **26**, 786–793 (1925).
8. Eland, J. H. D. The origin of primary H_3^+ ions in mass spectra. *Rapid Commun. Mass Spectrom.* **10**, 1560–1562 (1996).
9. De, S., Rajput, J., Roy, A., Ghosh, P. N. & Safvan, C. P. Formation of H_3^+ due to intramolecular bond rearrangement in doubly charged methanol. *Phys. Rev. Lett.* **97**, 213201 (2006).
10. Zhang, Y. et al. Formation of H_3^+ from ethane dication induced by electron impact. *Commun. Chem.* **3**, 160 (2020).
11. Wang, E., Ren, X. & Dorn, A. Role of the environment in quenching the production of H_3^+ from dicationic clusters of methanol. *Phys. Rev. Lett.* **126**, 103402 (2021).
12. Furukawa, Y., Hoshina, K., Yamanouchi, K. & Nakano, H. Ejection of triatomic hydrogen molecular ion from methanol in intense laser fields. *Chem. Phys. Lett.* **414**, 117–121 (2005).
13. Livshits, E., Luzon, I., Gope, K., Baer, R. & Strasser, D. Time-resolving the ultrafast H_2 roaming chemistry and H_3^+ formation using extreme-ultraviolet pulses. *Commun. Chem.* **3**, 49 (2020).
14. Okino, T. et al. Coincidence momentum imaging of ultrafast hydrogen migration in methanol and its isotopomers in intense laser fields. *Chem. Phys. Lett.* **423**, 220–224 (2006).
15. Hoshina, K., Furukawa, Y., Okino, T. & Yamanouchi, K. Efficient ejection of H_3^+ from hydrocarbon molecules induced by ultrashort intense laser fields. *J. Chem. Phys.* **129**, 104302 (2008).
16. Kraus, P. M. et al. Unusual mechanism for H_3^+ formation from ethane as obtained by femtosecond laser pulse ionization and quantum chemical calculations. *J. Chem. Phys.* **134**, 114302 (2011).
17. Kotsina, N., Kaziannis, S. & Kosmidis, C. Hydrogen migration in methanol studied under asymmetric fs laser irradiation. *Chem. Phys. Lett.* **604**, 27–32 (2014).
18. Ekanayake, N. et al. Substituent effects on H_3^+ formation via H_2 roaming mechanisms from organic molecules under strong-field photodissociation. *J. Chem. Phys.* **149**, 244310 (2018).
19. Ekanayake, N. et al. Mechanisms and time-resolved dynamics for trihydrogen cation (H_3^+) formation from organic molecules in strong laser fields. *Sci. Rep.* **7**, 4703 (2017).
20. Ekanayake, N. et al. H_2 roaming chemistry and the formation of H_3^+ from organic molecules in strong laser fields. *Nat. Commun.* **9**, 5186 (2018).
21. Ando, T., Iwasaki, A. & Yamanouchi, K. Strong-field Fourier transform vibrational spectroscopy of D_2^+ using few-cycle near-infrared laser pulses. *Phys. Rev. Lett.* **120**, 263002 (2018).
22. Alghabra, M. S. et al. Anomalous formation of trihydrogen cations from water on nanoparticles. *Nat. Commun.* **12**, 3839 (2021).
23. Knee, L. B. G. & Brunt, C. M. A massive cloud of cold atomic hydrogen in the outer Galaxy. *Nature* **412**, 308–310 (2001).
24. Duley, W. W. The formation of H_2 by H-atom reaction with grain surfaces. *Mon. Not. R. Astron. Soc.* **279**, 591–594 (1996).
25. Fletcher, L. N., Gustafsson, M. & Orton, G. S. Hydrogen dimers in giant-planet infrared spectra. *Astrophys. J. Suppl. Ser.* **235**, 24 (2018).
26. Mckellar, A. R. W. Possible identification of sharp features in the Voyager far-infrared spectra of Jupiter and Saturn. *Can. J. Phys.* **62**, 760–763 (1984).
27. Frommhold, L., Samuelson, R. & Birnbaum, G. Hydrogen dimer structures in the far-infrared spectra of Jupiter and Saturn. *Astrophys. J.* **283**, L79–L82 (1984).
28. Gibb, B. C. Chemistry of the sky god. *Nat. Chem.* **12**, 974–976 (2020).
29. Ullrich, J. et al. Recoil-ion and electron momentum spectroscopy: reaction-microscopes. *Rep. Prog. Phys.* **66**, 1463–1545 (2003).
30. Bucksbaum, P. et al. Softening of the H_2^+ molecular bond in intense laser fields. *Phys. Rev. Lett.* **64**, 1883–1886 (1990).
31. Sussman, B. J., Townsend, D., Ivanov, M. Y. & Stolow, A. Dynamic Stark control of photochemical processes. *Science* **314**, 278–281 (2006).

Methods

Ab initio molecular dynamics simulation

Ab initio molecular dynamics simulation is a technique that allows for the simulation of molecular systems and processes from first principles. The simulation was performed under the extended Lagrangian molecular dynamics scheme in which the atom-centred density matrix propagation (ADMP) approach and density functional theory (ωb97xd/aug-cc-pVDZ) were applied[32–35]. The details are described in Supplementary Sections 2 and 3, and only a brief introduction is provided here. The initial molecular configuration, that is, the geometries and the velocities of every atom of the D_2 dimer, were calculated by the Wigner distribution, which traverses all possible regions on the PES of the D_2 dimer. We assumed a vertical ionization from the neutral to cationic state of the D_2 dimer, and the sampled geometry and velocity were used for the initial configuration of the molecular dynamics simulation of the cationic state of the D_2 dimer. In the ADMP simulation, the fictitious electron mass was 0.1 AMU, and the simulation time step was 0.5 fs. Due to the low potential energy barrier of the D_2 dimer, the anharmonic effect in the sampling cannot be ignored. By comparing the sampled internuclear distance distribution and the ab initio potential energy curve (Supplementary Section 3), we find that the anharmonicity of the intermolecular potential leads to 7% of our trajectories to start inside the inner classical turning point. The molecular dynamics simulation showed that these events result in the same dissociation limit and may result in a shorter formation time for D_3^+.

Experimental set-up

In the reaction microscope, the backing pressure of the nozzle was 3 bar, and the D_2 gas in the nozzle was precooled to 60 K. The molecular beam intersects with a focused near-infrared laser beam (central wavelength $\lambda = 790$ nm, pulse duration $\tau = 25$ fs, repetition rate $f = 10$ kHz), where the ionization occurs. A static electric field (16 V cm^{-1}) guides the ions to a delay-line detector, which records the flight time and impact position for every produced ion. This allows reconstruction of the three-dimensional momenta and the kinetic energies for every detected charged particle. In our experiment, circularly polarized laser pulses with a peak intensity of 3×10^{14} W cm^{-2} are used to ionize D_2 dimers. With this intensity and the very low gas density in the reaction region, the overall count rate of photoions in the experiment was below 0.2 ions per laser pulse, resulting in a high-quality coincidence measurement.

Data availability

The data that support the findings of this study and the raw data for all the figures have been uploaded to Figshare[36] at https://doi.org/10.6084/m9.figshare.21509769. Source data are provided with this paper.

Code availability

The code for the ab initio molecular dynamics simulation is available from the corresponding author upon reasonable request.

References

32. Frisch, M. J. et al. Gaussian 16, Revision C.01 (Gaussian, 2016).
33. Schlegel, H. B. et al. Ab initio molecular dynamics: propagating the density matrix with Gaussian orbitals. *J. Chem. Phys.* **114**, 9758–9763 (2001).
34. Iyengar, S. S. et al. Ab initio molecular dynamics: propagating the density matrix with Gaussian orbitals. II. Generalizations based on mass-weighting, idempotency, energy conservation and choice of initial conditions. *J. Chem. Phys.* **115**, 10291–10302 (2001).
35. Schlegel, H. B. et al. Ab initio molecular dynamics: propagating the density matrix with Gaussian orbitals. III. Comparison with Born-Oppenheimer dynamics. *J. Chem. Phys.* **117**, 8694–8704 (2002).
36. Mi, Y. et al. Observation and dynamic control of a new pathway of H_3^+ formation (figshare, 2022); https://doi.org/10.6084/m9.figshare.21509769

Acknowledgements

We thank A. R. W. McKellar, A. Stolow, P. Bunker and T. Pfeifer for fruitful discussions. We acknowledge support from the Joint Centre for Extreme Photonics. Y.M. acknowledges support from the Deutsche Forschungsgemeinschaft (German Research Foundation) grant no. MI 2434/1-1 (Y.M.). E.W. is supported by the Strategic Priority Research Program of the Chinese Academy of Sciences, grant no. XDB34020000 (E.W.), and the Alexander von Humboldt Foundation. Financial support from the National Science and Engineering Research Council Discovery (grant no. RGPIN-2020-05858, A.S.) and from the US Air Force Office of Scientific Research (grant no. FA9550-16-1-0109, P.C.) is gratefully acknowledged.

Author contributions

Y.M. designed and conducted the experiments. E.W. performed molecular dynamics simulations. Z.D., A.Y.N. and A.S. assisted with the experiments. Y.M. and A.S. analysed the experimental data. Y.M., E.W. and A.S. wrote the manuscript with contributions from all other authors.

Competing interests

The authors declare no competing interests.

Additional information

Extended data is available for this paper at https://doi.org/10.1038/s41557-023-01231-z.

Supplementary information The online version contains supplementary material available at https://doi.org/10.1038/s41557-023-01231-z.

Correspondence and requests for materials should be addressed to Yonghao Mi, Enliang Wang or André Staudte.

Peer review information *Nature Chemistry* thanks Marcos Dantus and the other, anonymous, reviewer(s) for their contribution to the peer review of this work.

https://doi.org/10.1038/s41557-023-01231-z

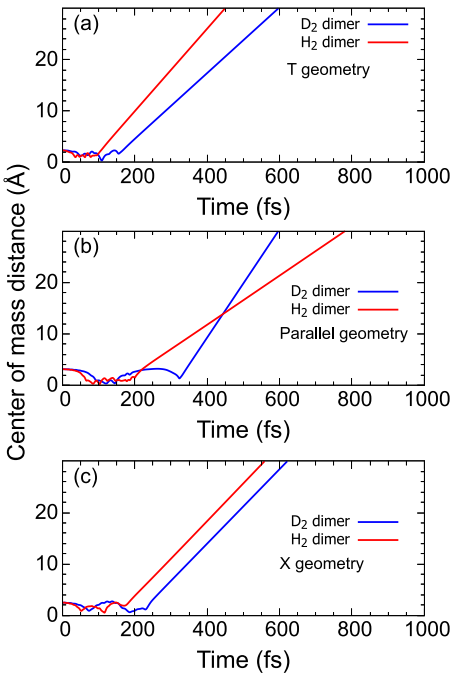

Extended Data Fig. 1 | Comparisons of the simulated center of mass distance as a function of time for the H_2 and D_2 dimer. (**a**), (**b**), and (**c**) correspond to the T-shape geometry, parallel geometry and X-shape geometry of the H_2 (red curves) and D_2 (blue curves) dimers, respectively. The results show that all initial configurations lead to the formation of H_3^+ or D_3^+. The molecule begins to dissociate once the trajectory shows a linear increase of the center of mass distance as a function of time. These results indicate that the H_2 dimer dissociates faster than the D_2 dimer.

https://doi.org/10.1038/s41557-023-01231-z

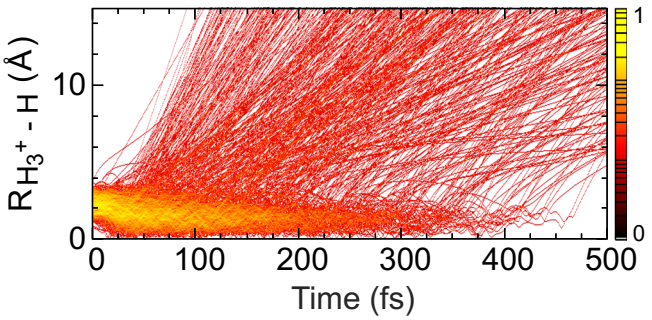

Extended Data Fig. 2 | Simulated trajectories of H_3^+ formation as a function of time. The simulated center of mass distance of $H_3^+ + H$ is shown for 493 trajectories, out of a total of 593 simulated trajectories for H_2–H_2. The branching ratio for this channel is 83.1%, which is very close to that of the $D_3^+ + D$ channel (89.2%).

https://doi.org/10.1038/s41557-023-01231-z

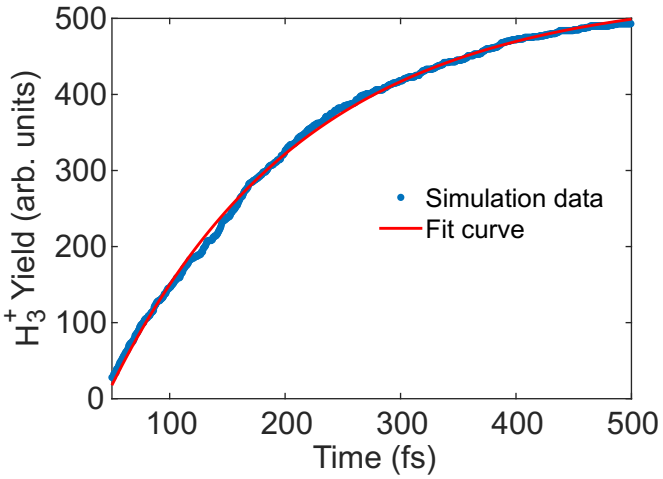

Extended Data Fig. 3 | Simulated time-dependent H_3^+ yield. The simulated data is obtained by projecting the trajectories with a center-of-mass distance larger than 4.2 Å onto the time axis, which excludes most of the oscillation structures. The red curve represents a fit to the data using the growth function $Y(t) = a(1\text{-}e^{-t/\tau}) + Y_0$, where a and Y_0 represent the amplitude and the offset of the H_3^+ yield, respectively, and τ is the formation time of H_3^+. By using this fit function, we find the formation time of H_3^+ is 169.5 fs.